JOURNAL OF MATERIALS SCIENCE **39** (2004) 2073–2080

A study of combustion synthesis reaction in the Ti + C/Ti + Al system

CHYI-CHING HWANG*
Department of Applied Chemistry, Chung Cheng Institute of Technology, Dashi Jen, Taoyuan, Taiwan 335, Republic of China
E-mail: cchwang1@ccit.edu.tw

SHYAN-LUNG CHUNG
Department of Chemical Engineering, National Cheng Kung University, Tainan, Taiwan 700, Republic of China

Combustion synthesis (SHS) of the Ti + C/Ti + Al system was investigated by using titanium, graphite and aluminum powders as reactants. These powders were thoroughly mixed and pressed into cylindrical compacts, and heated in an argon atmosphere. The effects of the reactant composition and the heating rate were studied. The phase identification and morphology observation of the products were carried out by X-ray diffraction (XRD) and scanning electronic microscopy (SEM), respectively. XRD analysis showed that the products, in addition to the expected TiC/TiAl phases, also contained an appreciable amount of the ternary carbide (i.e., Ti_xAlC). The heating rate was found to strongly affect the extent of the combustion reaction. A possible reaction mechanism based on the experimental results was proposed to describe the whole process of the SHS reaction and the characteristic product morphology. It was considered that the ternary carbides may be formed by the peritectic reaction between TiC and the Ti–Al melt during the cooling stage after combustion.

1. Introduction

Titanium aluminides have considerable development potential as high temperature materials due to their low density, high strength and good oxidation resistance at elevated temperatures [1]. On the other hand, TiC is an extremely hard material and has a very high melting point [2]. Composite materials consisting of TiC and titanium aluminides are expected to find use in various structural, cutting tool and armor applications.

In this work, we investigated the use of the combustion synthesis (also known as self-propagating high-temperature synthesis (SHS)) method for the production of TiC/TiAl composites. SHS, originally developed in the former USSR [3], has been applied to synthesis of various high-temperature materials including ceramics, intermetallics, and composites [4]. It has many potential advantages such as low processing cost, energy-efficiency and high production rate [5].

Many studies [6–8] have reported that the TiC/Al composite can be produced from a blend of Ti + C powders (in a molar ratio of 1:1) and Al powder via SHS, and the as-synthesized product is composed of TiC, Al and residual C. Recently, the synthesis of TiC/TiAl composite by combustion reactions involving Ti + C and Ti + Al has also been studied [9–12]. Ohyanagi *et al.* [9] claimed that SHS enabled synthesis of $TiC/TiAl_x$ composite and the product consisted of TiC, $TiAl_3$, TiAl and Ti_3Al. Therefore, at first sight, it seems that the TiC/Al and TiC/TiAl composites may be produced by SHS, using Ti + C/Al and Ti + C/Ti + Al as the reactants, respectively. However, the work of other researchers [10–12] on the SHS production of TiC/TiAl composite produced contradicting results. In their studies, the as-synthesized product was not the simple composite of TiC/TiAl as expected, but rather contained an appreciable amount of $Ti_4Al_2C_2$.

Although there have been some attempts to obtain TiC/TiAl composites through the SHS reaction, little information is available on the effect of processing conditions. Hence, this work examines the effects of reactant composition and heating rate on the combustion synthesis reaction of the Ti + C/Ti + Al system. The phase identification, microstructure observation and composition analysis were also carried out during and after the combustion reaction. Based on the experimental results, a possible reaction mechanism was thus proposed.

2. Experimental procedure

Listed in Table I are the characteristics of the reagents used in the present study. The titanium, graphite and aluminum powders were mixed to produce the

*Author to whom all correspondence should be addressed.

TABLE I The characteristics of the reagents used in the present study

Reagent	Particle size (μm)	Purity (%)	Source
Titanium	<45	99.5	Cerac, Milwaukee, WI
Graphite	<45	99.9	Carbon Cement Co., Tokyo, Japan
Aluminum	<45	99.7	Cerac, Milwaukee, WI

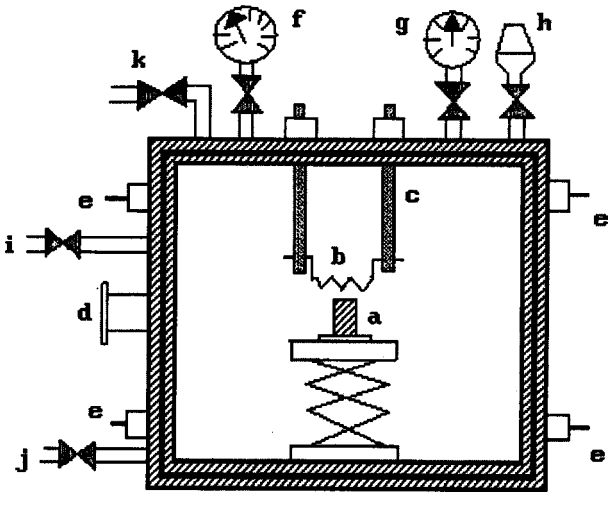

Figure 1 Schematic diagram of the reaction chamber: (a) reactant compact, (b) tungsten coil, (c) graphite rod, (d) observation window, (e) thermocouple lead, (f) pressure gauge, (g) vacuum gauge, (h) vacuum gauge tube, (i) gas inlet, (j) vacuum port, and (k) vent.

stoichiometric compositions of TiC and TiAl (i.e., both in an atomic ratio of 1:1). The powders were mixed to provide a varying weight ratio of Ti + C/Ti + Al in a range from 10/90 to 90/10 (the weight ratio of Ti + C/Ti + Al is hereafter referred to as R). The reactant powders were thoroughly mixed in the presence of an organic solvent. After drying in vacuum, 2.5 g of the reactant powders were pressed into cylindrical compacts (referred to as reactant compacts) 10 mm in diameter and ~12 mm in length. A stainless steel die with two plungers was used and a pressure of ~100 MPa was uniaxially applied to form the reactant compacts.

Fig. 1 shows the schematic diagram of the reaction chamber used in the present study. The reactant compact was placed on a height-adjustable stage in the reactor. The stage was adjusted so that the top surface of the reactant compact was approximately 4 mm below the tungsten filament. The reactor was evacuated to 65 Pa and flushed with argon between evacuations and back-filled with argon at 0.1 MPa. The combustion reaction was carried out by heating the top surface of the reactant compact by passing an electric current (20–80 V, 15–30 A) through the tungsten filament. The electrical power was turned off right after ignition. The temperatures were measured by using 0.127 mm diameter W-3%Re/W-25%Re thermocouples insulated with 1.2 mm diameter alumina tubes. Fig. 2 shows the configurations and the locations of the thermocouples. Thermocouple A was placed in a narrow groove (0.5 mm wide and 0.2 mm deep) cut into the top surface of the reactant compact to obtain the temperature profile during heating and ignition. Thermocouple B was inserted

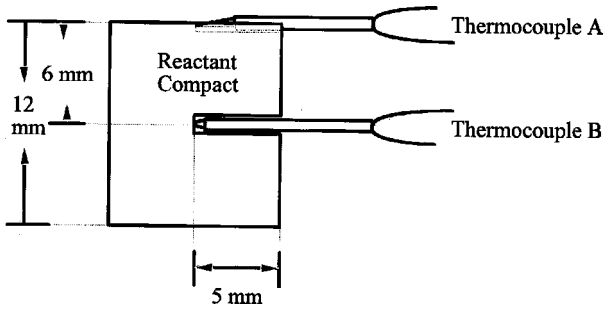

Figure 2 Configurations and locations of thermocouples for ignition and combustion temperatures measurements.

to the center of the reactant compact by first drilling to obtain temperature profile during combustion. The signals from the thermocouples were stored and processed by a data acquisition system. Combustion wave velocity was measured using a video camera at a speed of 30 frames/s.

The product identification was determined by X-ray diffraction (XRD) analysis (SIEMENS D5000, Germany) and the product morphology was examined with a scanning electron microscope (SEM, Topcon ABT-60, Japan). Elemental composition analyses were carried out by a wavelength dispersive X-ray spectrometry (WDS, Jeol JSM-35, Japan) and energy dispersive X-ray spectrometry (EDS, Jeol JED-2001, Japan).

3. Results and discussion

3.1. Effects of reactant composition

3.1.1. Measurement of temperature during SHS reactions

Typical temperature-time histories obtained by thermocouple A for reactant compacts with various compositions are shown in Fig. 3. The slope of each profile at the initial increase of temperature is defined as the heating rate. Taking the case of $R = 50/50$ as an example, the increase in temperature begins to slow down when the temperature reaches ~760°C, and at 920°C, the temperature increases rapidly up to ~1230°C and then its increase slows down again until the temperature reaches 1420°C, where the temperature increases abruptly. Since the abrupt increase in temperature is accompanied by luminous light emission due to onset of the combustion reaction, the temperature at the point

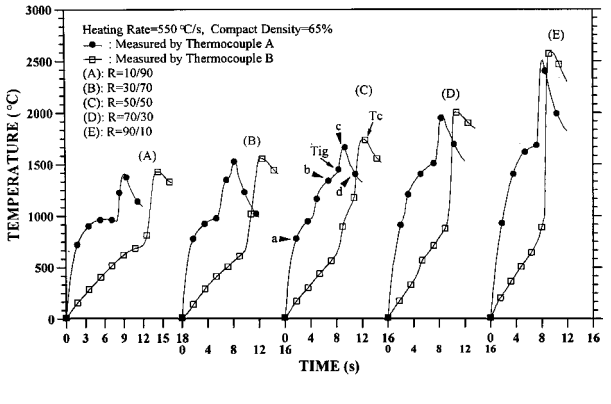

Figure 3 Typical temperature-time histories during heating and reaction for reactant compact with various composition.

of abrupt increase is defined as the ignition temperature (T_{ig}). The temperature-time histories for the two cases of $R = 30/70$ and 70/30 are similar to that of $R = 50/50$. Two exothermic peaks are also observed, and the ignition temperatures are found to be 1410°C and 1540°C. With a decreasing value of R, the lower exothermic peak becomes easier to detect, while the opposite happens for the second one. In the two cases of $R = 90/10$ and $R = 10/90$, only one exothermic peak was recorded. The combustion reaction for the compact of $R = 90/10$ ignited at 1620°C, while that for $R = 10/90$ ignited at 900°C. It is found that the ignition temperature decreases with decreasing R value. From the relations between the reactant compositions and the temperature-time histories, it seems that the first peak is caused by the reaction of Ti + Al whereas the second peak is caused by the formation of TiC (will be explained later).

As also shown in Fig. 3, the combustion temperature (i.e., the maximum temperature measured by thermocouple B) increases with increasing R value and ranges between 1480°C and 2512°C. Since the heat of formation of TiC is more negative than that for the Ti—Al intermetallics [9], the combustion temperature increases with increasing the content of Ti + C.

3.1.2. XRD analysis

Fig. 4 shows the XRD patterns of the products synthesized from reactant compacts with various compositions. The products of $R = 10/90$ and 30/70 both contain two kinds of titanium aluminides, i.e., TiAl and Ti_3Al and one ternary carbide, i.e., $Ti_4Al_2C_2$. In the cases of $R = 90/10$ and 70/30, both products are composed of TiC and two kinds of ternary carbides, i.e., $Ti_4Al_2C_2$ and Ti_3AlC. For the composition of $R = 50/50$, the product is composed of TiAl, Ti_3Al and three kinds of ternary carbides, i.e., TiC, $Ti_4Al_2C_2$ and Ti_3AlC.

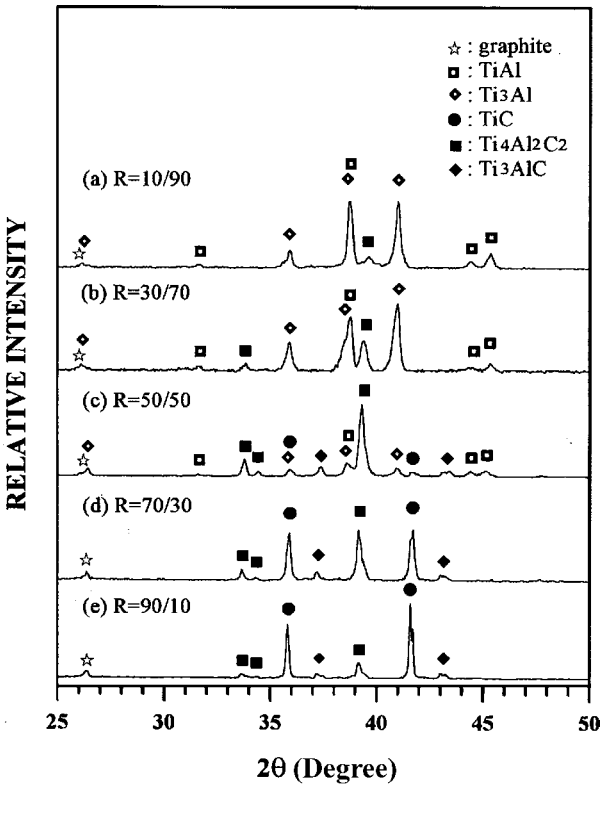

Figure 4 XRD patterns of the products synthesized from reactant compacts with various compositions.

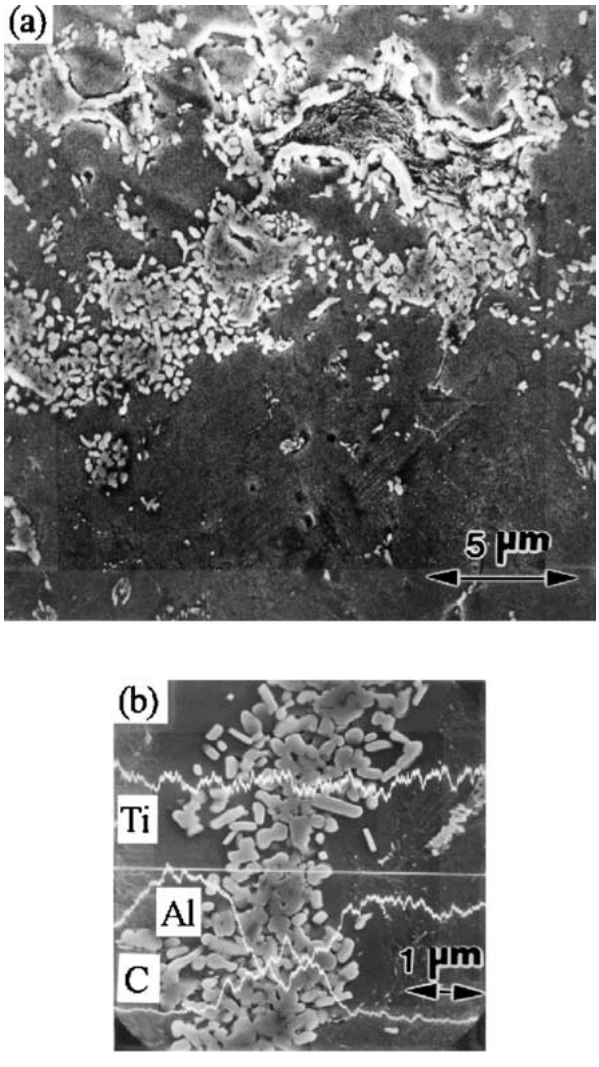

Figure 5 (a) Typical SEM photograph of the polished surface of the product synthesized with the reactant composition of $R = 10/90$. (b) Results of the WDS line analysis of the same sample shown in Fig. 5a.

3.1.3. Product morphology

Shown in Fig. 5a is a typical SEM photograph of the polished surface of the product synthesized with the composition of $R = 10/90$. As can be seen, the product consists of rod-shape grains (approximately 0.2 μm wide and 0.5 μm long), a matrix phase and residual reactant particles. Fig. 5b presents the results of WDS line analysis. The Ti analysis line reveals that the Ti content is slightlt higher in the matrix phase than in the rod-shape grains. However, the Ti analysis line shows minor fluctuations of the Ti concentration when compared with C and Al analysis lines, which are conceivably uncorrelated with the product materials being scanned. The C analysis line indicates that the C content increases as it enters the rod-shape grains, while the Al analysis line indicates that the Al content is higher in the

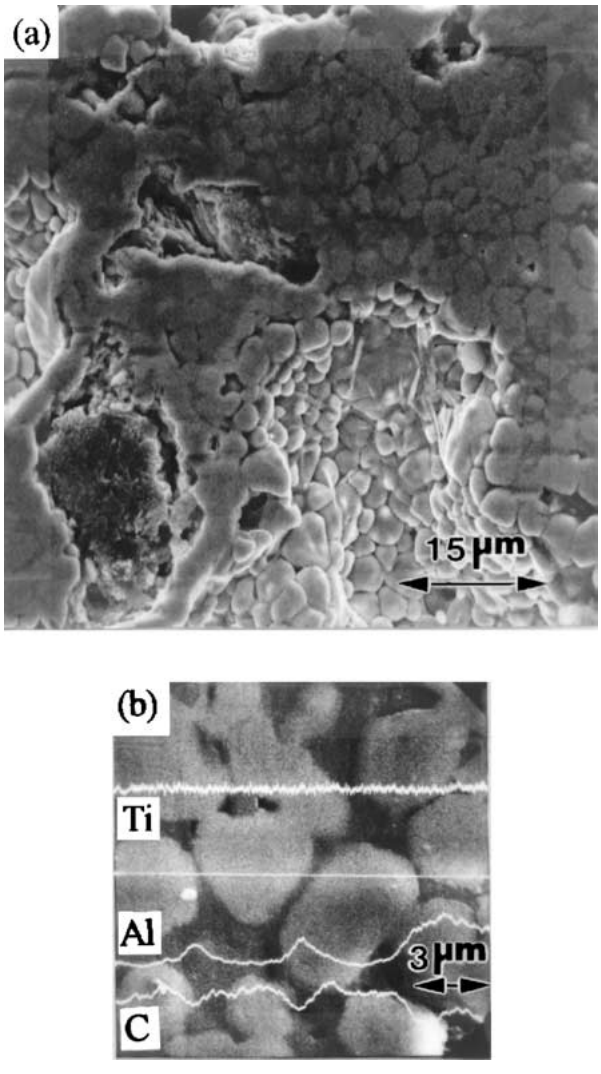

Figure 6 (a) Typical SEM photograph of the polished surface of the product synthesized with the reactant composition of $R = 90/10$. (b) Results of the WDS line analysis of the same sample shown in Fig. 6a.

matrix phase than in the rod-shape grains. This result, coupled with the XRD analysis (Fig. 4a), suggests that the rod-shape grains are $Ti_4Al_2C_2$ and the matrix phase consists of TiAl and Ti_3Al. The residual reactant particle was identified as graphite by WDS point analysis. Similar morphology and WDS analysis results were also obtained from the product synthesized with the composition of $R = 30/70$.

Shown in Fig. 6a is a typical SEM photograph of the polished surface of the product synthesized with the composition of $R = 90/10$. The product consists of discrete grains (2–8 μm in diameter) surrounded by a dark-colored phase and residual reactant particles. Fig. 6b shows the results of WDS line analysis of the same sample. The Ti analysis line exhibits an essentially unchanged concentration of Ti when scanning across the grain and the dark-colored phase. The Al analysis line indicates that the Al content is lower in the discrete grains than in the dark-colored phase, whereas the opposite is revealed by the C analysis line. Since only TiC and two ternary carbides ($Ti_4Al_2C_2$ and Ti_3AlC) were detected in the XRD analysis (Fig. 4e), it is suggested that the discrete grains are TiC and the dark-colored phase is composed of the two ternary carbides. The residual reactant particles were identified as graphite by WDS point analysis. Similar morphology and results of WDS analysis were also obtained from the product synthesized with the composition of $R = 70/30$.

TABLE II Results of elemental composition analyses of the product synthesized with the reactant composition of $R = 50/50$ and a heating rate of 550°C/s

	WDS[a] (count)			EDS (at.%)	
Morphology	Ti	Al	C	Ti	Al
Fine particle	2145	87	822	95.1	4.9
Rod-shape grain	2071	2862	626	68.3	31.7
Granular crystal	2370	2287	514	73.6	26.4
Continuous phase	2217	2740	44	70.8	29.2
Unreacted particle	68	92	3473	–	–

[a]An accelerating voltage of 12 kV, a regulated beam current of about 6 nA and a counting time of 20 s were selected as standard operating conditions.

Fig. 7a is a typical SEM photograph of the polished surface of the product synthesized with the composition of $R = 50/50$. The product is seen to consists of discrete particles, a continuous phase and residual reactant particles. The discrete particles can be classified into three types according to their morphologies, i.e., fine particles ($\sim$1 μm in diameter, Fig. 7b), rod-shape grains ($\sim$0.5–1.5μm wide and $\sim$ 6–10 μm long, Fig. 7c) and granular crystals (3–7μm, Fig. 7d). Table II shows the results of elemental composition analysis of the same sample. These results associated with the XRD analysis (Fig. 4c) indicates that the fine particles are TiC, the rod-shape grains are $Ti_4Al_2C_2$, the granular crystals are Ti_3AlC, the continuous phase is composed of TiAl and Ti_3Al intermetallic compounds and that the residual reactant particles are graphite.

3.2. Reaction mechanism

In the present study, the product is not a simple composite mixture of TiC/TiAl, but the ternary carbide exists in the final products. In order to develop an understanding of the chemical reactions occurring during the process of SHS, four reactant compacts with the same composition of $R = 50/50$ were heated using a heating rate of 550°C/s and the temperature at the top of the compacts recorded (using the thermocouple A). These reactant compacts were rapidly quenched when the temperatures reached the values at a, b, c, and d marked in Fig. 3, respectively. The top surface of each sample was then analyzed by XRD and the results are shown in Fig. 8. As shown in the XRD pattern (a), there was no evidence of compound formation before the first exothermic peak (point a in Fig. 3). After the first exothermic peak (point b in Fig. 3), three Ti–Al compounds formed, while all the Al had been consumed, but some unreacted Ti remained (the XRD pattern (b)). TiC was formed (XRD pattern (c)) after ignition of the compact (point c in Fig. 3). The ternary carbides, i.e., $Ti_4Al_2C_2$ and Ti_3AlC were formed (XRD pattern (d)) during the cooling stage (point d in Fig. 3).

Figs 8a–c represent the different stages of the phase formation during the early period of the whole SHS

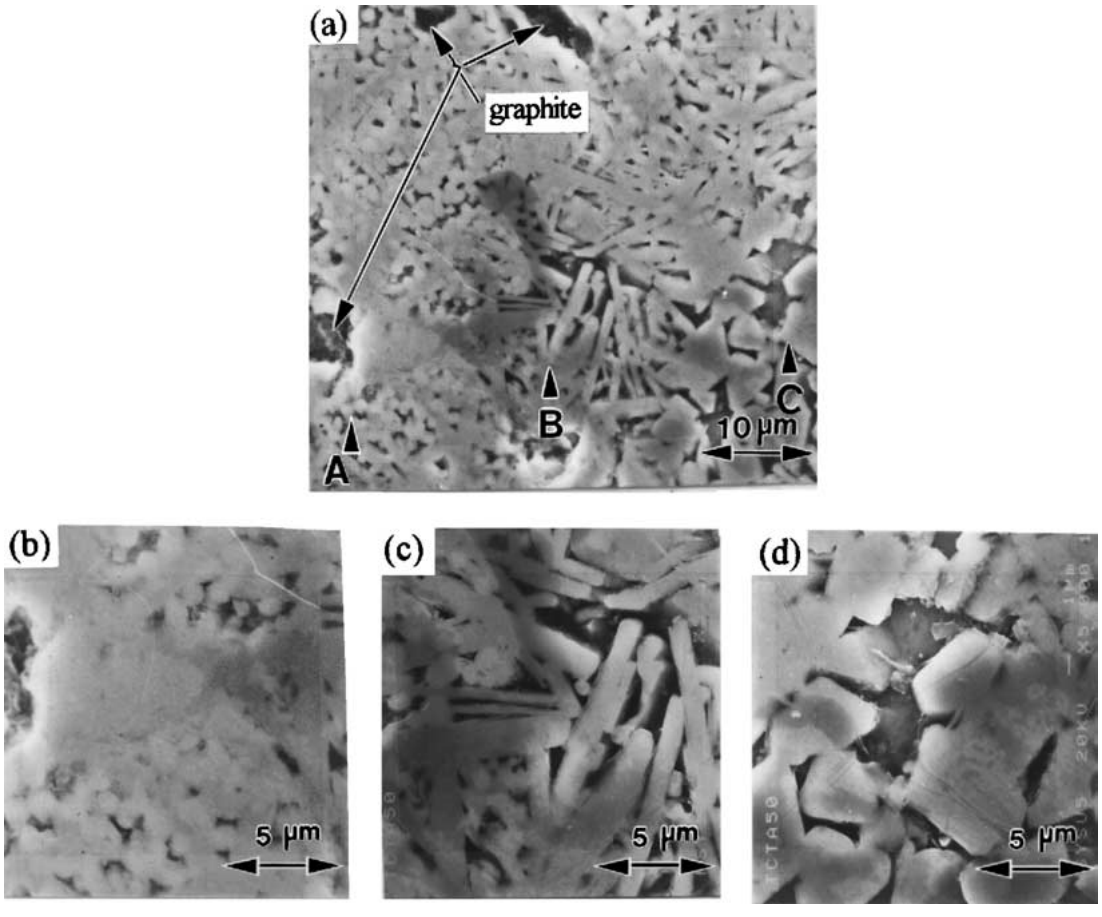

Figure 7 (a) Typical SEM photograph of the polished surface of the product synthesized with the reactant composition of $R = 50/50$. (b) Notion "A" in Fig. 7a, showing fine particles. (c) Notion "B" in Fig. 7b, showing rod-like structures. (d) Notion "C" in Fig. 7c, showing granular grains.

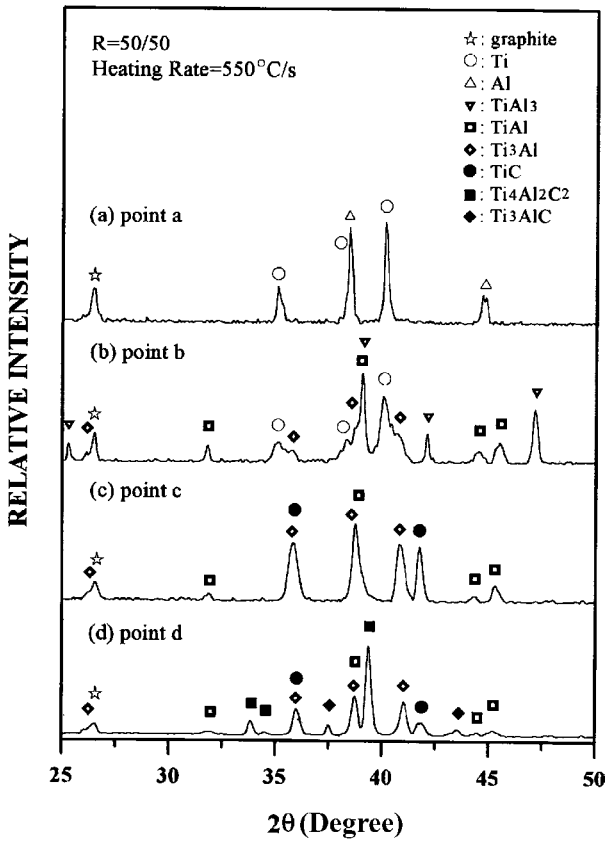

Figure 8 Results of XRD analysis of the top surfaces of the reactant compacts. (Four samples with the same composition of $R = 50/50$ were heated to different temperatures, marked *a*, *b*, *c*, and *d*, and then quenched.)

reaction with the composition of $R = 50/50$. The result is in agreement with the previous study by Lee and Chung [6], in which TiC/Al composite was synthesized by combustion reaction. Upon heating, Al melts and preferentially reacts with Ti to form $TiAl_x$ compounds as the temperature reaches the melting point of Al. The exothermic reaction between Ti and molten Al gives rise to the first exothermic peak (e.g., $\Delta_f H^0_{TiAl_3} = -142.26$ KJ/mol, $\Delta_f H^0_{TiAl} = -72.80$ KJ/mol). As the temperature is further increased, the $TiAl_x$ compounds melt and a liquid phase containing Ti can be produced. Many studies [7, 13–16] have revealed that TiC can be formed spontaneously by the reaction of graphite with the Ti contained in the Ti–Al melt. TiC is thus formed by the highly exothermic reaction between graphite particles and the Ti–Al melt ($\Delta_f H^0_{TiC} = -186$ KJ/mol). Consequently, the ignition occurs and results in the second exothermic peak. However, comparing Fig. 8c and d, an appreciable amount of TiC was formed prior to the formation of the ternary carbide. This was followed by a reduction of the quantity of TiC and the titanium aluminides , while the ternary carbide became predominant. This result implies that the ternary carbides may be formed by reaction between TiC and $TiAl_x$.

In order to confirm this suggestion, four compacts with the compositions of 30 wt%TiC + 70 wt%Al, 30 wt%TiC + 70 wt% (Ti + 3Al), 30 wt%TiC+70 wt% (Ti + Al) and 30 wt%TiC+ 70 wt% (3Ti + Al) were prepared. These compacts were heated and kept at ∼1500°C for 30 s in an argon atmosphere to produce the

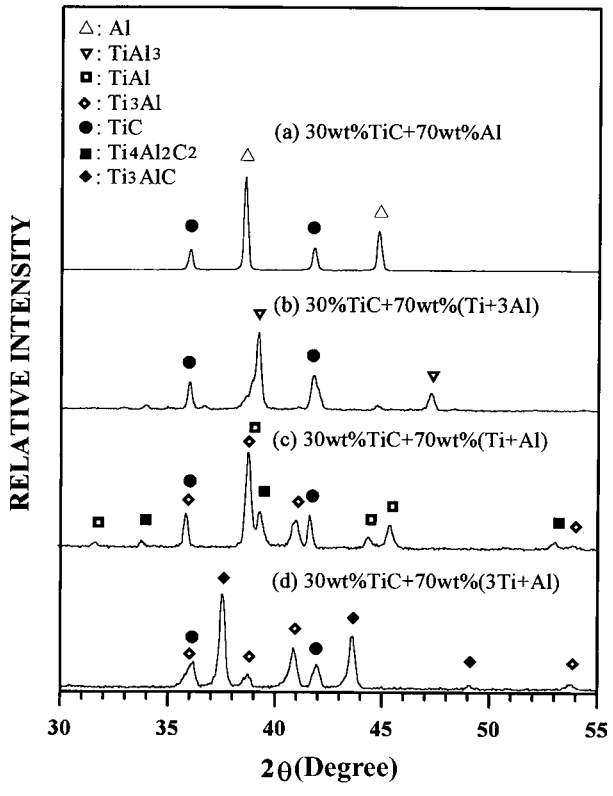

Figure 9 XRD patterns of the top surfaces of various TiC-Ti-Al reactant compacts heated at 1500°C for 30 s.

melts containing various Ti content and to simulate the circumstances during the combustion reaction. (Note that the combustion temperature increases with increasing R value and ranges between 1480 and 2512°C (see Fig. 3). From the phase diagram of the Ti–Al system [17], the Ti—Al melt will be present in the temperature range.) Fig. 9 shows no evidence of ternary carbide formation in the products from the 30 wt% TiC+70 wt%Al and 30 wt%TiC+70 wt% (Ti+3Al) compacts, while the 30 wt%TiC+70 wt% (Ti + Al) and 30 wt%TiC+70 wt% (3Ti + Al) compacts produced appreciable amounts of $Ti_4Al_2C_2$ and Ti_3AlC, respectively. Kennedy *et al*. [18] investigated the reactions in Al-10 wt% TiC metal matrix composites prepared using a casting technique. They found that the reaction between TiC and Al is possible to occur below about 900°C, and thus to form $TiAl_3$ and Al_4C_3. However, our experimental result indicates that at ~1500°C liquid Al and the aluminium-rich Ti–Al melt do not react with TiC. This result may also explain why no ternary carbide phase exists in the TiC/Al composite synthesized via SHS, since TiC seems stable in molten Al. When the Ti content increased to a certain extent, TiC reacted with the Ti–Al melt to form the $Ti_4Al_2C_2$ phase. However, the Ti_3AlC phase was produced when the Ti–Al melt contained an even higher Ti content. Evidence can be found from the morphology of the products to support this suggestion. In the case of lower R values (i.e., a higher Ti + Al content), $Ti_4Al_2C_2$ particles are dispersed in the matrix of titanium aluminides (see Fig. 4a), since TiC can react with a greater amount of Ti–Al melt and convert to the $Ti_4Al_2C_2$ phase. In the case of a higher Ti + C content (i.e., a higher R value), the relatively smaller amount of Ti–Al melt spreads over the TiC grain after the combustion, and the reaction occurs. Consequently the ternary carbide layer is formed on the surface of TiC (see Fig. 6a). Since TiC can be formed spontaneously by the reaction of graphite with the Ti contained in the Ti–Al melt, Ti is specifically consumed in the vicinity of graphite particle. The Ti content of the Ti–Al melt should increase with increasing the distance to the graphite particle. In the product synthesized from $R = 50/50$ sample (see Fig. 7a), the TiC particles are found in the vicinity of the graphite particle where the Ti concentration is low. Since the activity of Ti–Al melt becomes too low, the reaction between TiC and Ti–Al melt does not proceed. At the locations where the Ti concentration is high (i.e., far from the graphite particle), Ti_3AlC is formed by reaction of TiC with the melt containing a high Ti content. At other locations where the Ti concentration is moderate, the reaction between TiC and the Ti–Al melt leads to the formation of $Ti_4Al_2C_2$. Since this suggestion is consistent and matches with the experimental observations, it is confirmed that the ternary carbides may be formed by a peritetic reaction between TiC and the Ti–Al melt during the cooling stage after combustion.

3.3. Effects of heating rate

Fig. 10 shows the effects of the heating rate on the ignition temperature, the combustion temperature and the combustion wave velocity with a reactant composition of $R = 50/50$. At low heating rates (<300°C/s, zone I in Fig. 10), the reactant compact could not be ignited. A typical temperature-time history measured by thermocouple A is shown in Fig. 11. Only one exothermic peak was recorded, which is followed by a plateau showing a thermal steady-state. Obviously, the temperature of the top surface of the reactant compact cannot increase continuously to a sufficiently high value to ignite the whole combustion reaction.

In the heating rate range of 300–450°C/s (zone II in Fig. 10), the reactant compact could be ignited, however, the combustion wave ceased before it reached the end of the compact. Shown in Fig. 12 is a typical SEM

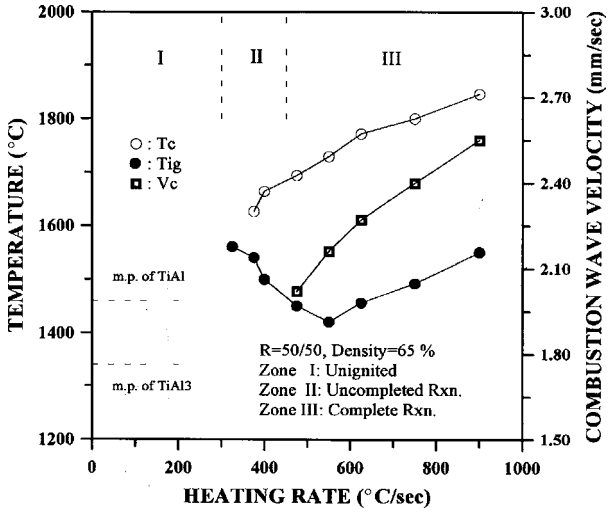

Figure 10 Effect of heating rate on igniting temperature, combustion temperature, and combustion wave velocity.

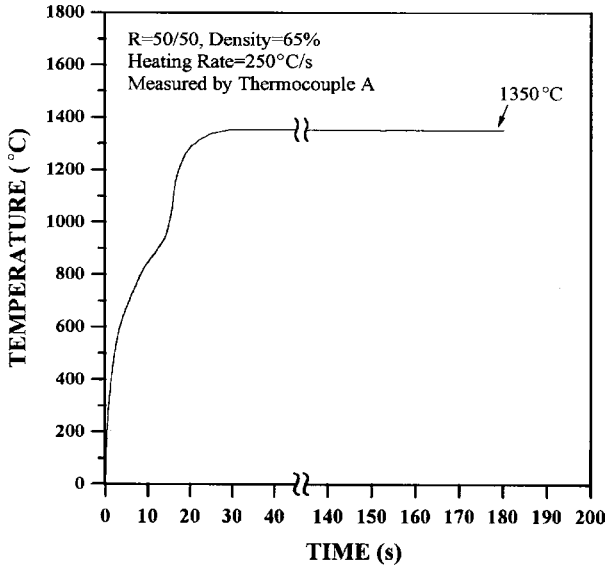

Figure 11 A typical time-temperature history measured by thermocouple *A* with the application of low heating rate.

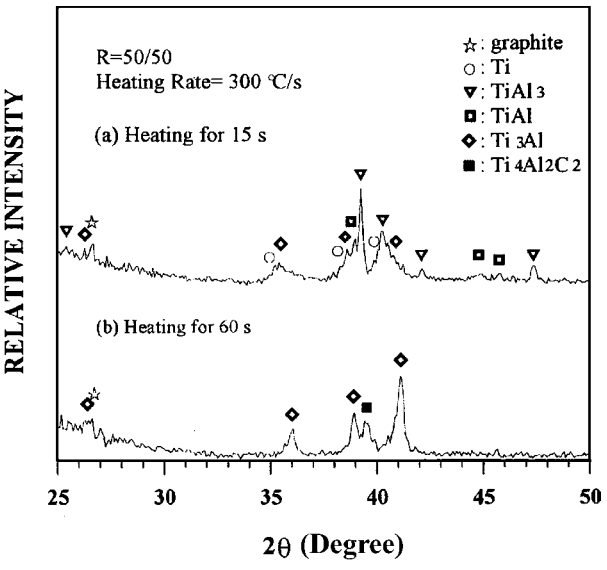

Figure 13 XRD patterns of the top surfaces of the reactant compacts after heating for (a) 15 and (b) 60 s, respectively.

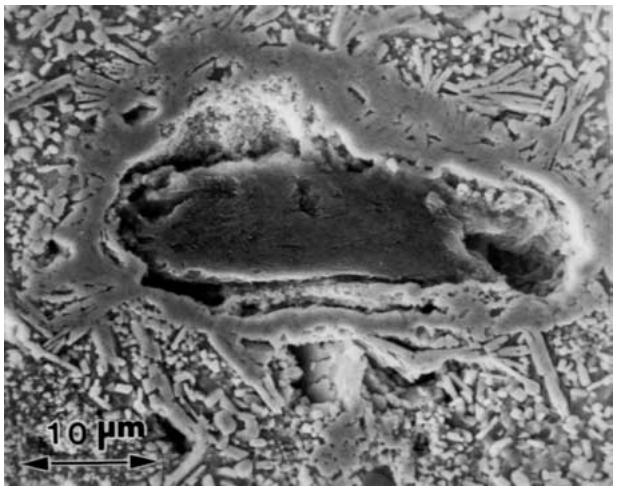

Figure 12 A Typical SEM photograph taken on the polished cross-section where the combustion wave ceased.

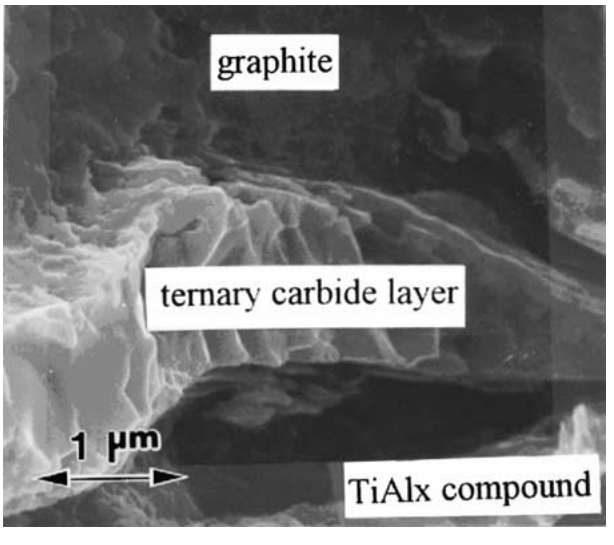

Figure 14 A high magnification SEM photograph of the top surface of the reactant compact after heating for 60 s with the application of a heating rate of 300°C/s, showing formation of the ternary carbide layer at the graphite/$TiAl_x$ interface.

photograph taken on the polished cross-section where the combustion wave ceased. A layer of dense substance (2–7μm in thickness) is observed to surround the graphite particle. This dense substance was identified as a mixture of TiC and $Ti_4Al_4C_4$ by elemental composition analysis. Two reactant compacts with the composition of $R = 50/50$ were heated at a lower heating rate (i.e., 300°C/s) and then quenched after heating, one for 15 s (just after the first exothermic peak) and the other for 60 s (before the ignition). The top surfaces of the reactant compacts were analyzed by XRD. These results are shown in Fig. 13. $TiAl_3$ was the primary product after the first exothermic peak. As the heating time increased to 60 s, Ti_3Al became predominant and a ternary carbide, i.e., $Ti_4Al_2C_2$ was also observed to form. Fig. 14 is a SEM micrograph of the top surface of the reactant compact that has been heated for 60 s. From the elemental composition analysis, as shown, a carbide layer was found to form at the interface between the graphite particle and the Ti–Al compound. Therefore, under a lower heating rate, the Ti-rich titanium aluminide and the carbide, i.e., $Ti_4Al_2C_2$ may be formed before the onset of ignition by solid-state diffusion. This result is similar to that found in the investigation by Viala *et al.* [17] who studied the high-temperature chemical interaction between carbon and titanium aluminides at 1000°C and observed that ternary carbide compounds can be formed at the interface between graphite and titanium aluminides. Under such circumstances, the $Ti_4Al_2C_2$ layer may act as both a kinetic barrier and a diluent, resulting in a higher ignition temperature and a lower combustion temperature. Consequently, the carbide layer grows to a thickness that significantly retards the reaction and causes the combustion reaction to extinguish (see Fig. 12).

In the case of a high heating rate (>450°C/s, zone III in Fig. 10), the combustion reaction of the entire reactant compact could be completed. As shown in Fig. 10, the ignition temperature (T_{ig}) decrease with increasing

heating rate to a minimum of 1420°C at a heating rate of 550°C/s and then begins to increase with further increase in the heating rate. This effect on the T_{ig} is similar to observations from a previous study [6]. Since the maximum extent of capillary spreading of the Ti–Al melt on the graphite particles and the rearrangement of the particles may not be reached when ignition occurs, a higher ignition temperature is required when applying a high heating rate in the high- heating-rate range (>600°C/s). In zone III the combustion temperature (T_c) and combustion wave velocity (v_c) both increase with increasing heating rate. Under such circumstances, since there is no reaction barrier arising from the carbide layer before the onset of ignition (see Fig. 8b), the higher ignition temperature may result in a higher combustion temperature which speeds up the combustion wave velocity as well. (theoretically, the combustion wave velocity increases exponentially with increasing combustion temperature [4]). On the other hand, a faster reaction rate (corresponding to a faster combustion wave velocity) may lower the amount of heat dissipated into the surroundings and thus raise the combustion temperature.

4. Conclusion

In this study, titanium, aluminum, and graphite powders are reacted by the combustion synthesis method in an attempt to obtain TiC/TiAl composites. However, the product is not the expectd composite of TiC/TiAl, but ternary carbides form in addition to titanium aluminides.

The ignition temperature and combustion temperature both increase with increasing R value (=Ti + C/Ti + Al). The product phases vary, depending on the reactant composition. The composites of $R = 10/90$ and 30/70, yield two kinds of titanium aluminides, i.e., TiAl and Ti_3Al and one ternary carbide, i.e., $Ti_4Al_2C_2$. In the cases of $R = 90/10$ and 70/30, the products are composed of three kinds of ternary carbides, i.e., TiC, $Ti_4Al_2C_2$ and Ti_3AlC. For the composition of $R = 50/50$, the product contains two kinds of titanium aluminides, i.e., TiAl and Ti_3Al and three kinds of carbides, i.e., TiC, $Ti_4Al_2C_2$ and Ti_3AlC. Based on the experimental observations, there was evidence that the ternary carbide may be formed by a peritectic reaction between TiC and the Ti–Al melt during the cooling stage after combustion.

Depending on the value of the heating rate, three characteristic zones can be identified in the case of $R = 50/50$, in which different reaction regimes are observed. The reactant compact can not be ignited below a heating rate of 300°C/s. In the heating range between 300–450°C/s, the combustion wave ceases before it reaches the end of the reactant compact. Under such circumstances, the ternary carbide may be formed by solid-state diffusion before ignition. Extinguishing of the combustion reactions may be accounted for by the formation of the carbide layer that acts both as a diluent and a reaction barrier. When the heating rate is higher than 450°C/s, the combustion reaction of the reactant compact could be completed. In this regime, the combustion temperature and combustion wave velocity both increase with increasing heating rate. The ignition temperature decreases with increasing heating rate to a minimum of 1420°C at 550°C/s and then increases with further increase in the heating rate.

Acknowledgment

Support for this research by the National Science Council of the Republic of China under Grant No. NSC 90-2214-E-014-002 is gratefully acknowledged.

References

1. F. H. FROES, C. SURYANARAYANA and D. ELIEZER, *J. Mater. Sci.* **27** (1992) 5113.
2. S. ADACHI, T. WADA, T. MIHARA, Y. MIYAMOTO, M. KOIZUMI and O. YAMADA, *J. Amer. Ceram. Soc.* **72** (1989) 805.
3. A. G. MERZHANOV and I. P. BOROVINSKAYA, *Combust. Sci. Technol.* **10** (1975) 195.
4. Z. A. MUNIR, *Ceram. Bull.* **67** (1988) 342.
5. J. F. CRIDER, *Ceram. Eng. Sci. Proc.* **3** (1982) 519.
6. W. C. LEE and S. L. CHUNG, *J. Amer. Ceram. Soc.* **80** (1997) 53.
7. Y. CHIO and S. W. RHEE, *J. Mater. Sci.* **28** (1993) 6669.
8. I. GOTMAN, M. J. KOCZAK and E. SHTESSEL, *Mater. Sci. Eng.* A **187** (1994) 189.
9. M. OHYANAGI, T. YOSHIKAWA, T. YAMAMOTO, M. KOIZUMI, S. HOSOMI, E. A. LEVASHOV, K. L. PADYUKOV and I. P. BOROVINSKAYA, in "Advanced Materials '93, I/A: Ceramics, Powders, Corrosion and Advanced Processing," edited by N. Mizutani *et al*., Trans. Mat. Res. Soc. Jpn., Vol. 14A (Elsevier Science B.V.) p. 685.
10. H. E. MAUPIN and J. C. RAWERS, *J. Mater. Sci. Lett.* **12** (1993) 540.
11. R. TOMOSHIGE and T. MATSUSHITA, *J. Ceram. Soc. Jpn.* **104** (1996) 93.
12. T. YAMASAKI, T.YAMAMOTO, K. N. ISBIBARA and H. P. SHINGU, *J. Jpn. Soc. Powder Powder Metall.* **47** (2002) 921.
13. M. J. KOCZAK and K. S. KUMAR, In-situ Process for Producing a Composite Containing Refractory Material, US patent no. 4,808,372, 1989.
14. S. KHATRI and M. J. KOCZAK, *Mater. Sci. Eng.* A **162** (1993) 153.
15. P. S. MOHANTY and J. E. GRUZLESKI, *Scripta Metallurgica et Materialia* **31** (1994) 179.
16. H. OKAMOTO, *J. Phase Equilibria* **1** (1993) 120.
17. J. C. VIALA, N. PEILLON, L. CLOCHEFERT and J. BOUIX, *Mater. Sci. Eng.* A **203** (1995) 222.
18. A. R. KENNEDY, D. P. WESTON and M. I. JONES, *ibid.* **316** (2001) 32.

Received 5 February
and accepted 3 December 2003